Electronic structure of MeS (Me = Ni,Co,Fe): x-ray absorption analysis

2004 J. Phys.: Condens. Matter 16 7545

(http://iopscience.iop.org/0953-8984/16/41/031)

INSTITUTE OF PHYSICS PUBLISHING JOURNAL OF PHYSICS: CONDENSED MATTER

J. Phys.: Condens. Matter **16** (2004) 7545–7556 PII: S0953-8984(04)82522-0

Electronic structure of MeS (Me = Ni, Co, Fe): x-ray absorption analysis

A V Soldatov[1,3], A N Kravtsova[1], M E Fleet[2] and S L Harmer[2]

[1] Faculty of Physics, Rostov State University, 5 Sorge, Rostov-on-Don, 344090, Russia
[2] Department of Earth Sciences, University of Western Ontario, London, ON, N6A 5B7, Canada

E-mail: soldatov@rsu.ru

Received 18 June 2004, in final form 2 September 2004
Published 1 October 2004
Online at stacks.iop.org/JPhysCM/16/7545
doi:10.1088/0953-8984/16/41/031

Abstract

The sulfur K and $L_{2,3}$ x-ray absorption near-edge structure (XANES) spectra of FeS, CoS and NiS having the NiAs-type crystal structure have been measured. Theoretical analysis of the experimental data has been conducted by the full multiple-scattering approach. Good agreement between experimental and theoretical data is obtained for comparatively small clusters containing 19–37 atoms. There is no significant difference between S K-edge absorption spectra for the studied compounds calculated by G4XANES and FEFF8.2 packages. The electronic structure of NiS and CoS has been studied by analysing the distribution of calculated electronic states of the sulfides.

1. Introduction

Iron, cobalt and nickel monosulfides have a hexagonal NiAs-type (B8) structure under ambient pressure and temperature. Their electronic structure is of interest in geochemistry and astrogeology, as well as in solid state physics and chemistry. The title compounds are represented in nature by pyrrhotite ($Fe_{1-x}S$), an important mineral in sulfide ore deposits and mine waste, troilite (FeS), the dominant sulfide of meteorites and lunar rocks, and the uncommon mineral jaipurite ($Co_{1-x}S$). Sugiura and co-workers [1–3] were the first to record the S K-edge, S Kβ x-ray emission and Fe K-edge absorption spectra of iron sulfides. The first multiple-scattering calculation of the S K-edge absorption spectra of FeS, CoS and NiS were performed by Kitamura *et al* [4]. The Fe K and $L_{2,3}$ and S K x-ray absorption edges of iron sulfides were recorded and discussed in terms of the calculated band structures by Womes *et al* [5]. The S K-edge XANES of the 3d transition monosulfides including FeS, CoS and NiS were recently investigated by Zajdel *et al* [6] and compared with linear muffin-tin orbital (LMTO)

[3] Author to whom any correspondence should be addressed.

numerical calculations. The S K-edge x-ray absorption spectra have been studied in Zn–(Mn, Fe, Co)–S systems [7] and ZnS, MnS, FeS and ZnFeS [8]. The Ni L-edge XANES of NiS has also been analysed [9]. We have measured S K-edge XANES of $(Fe, Co, Ni)_{0.923}S$ (B8 structure) solid solutions [10], and S K- and L-edge XANES of (Mn, Fe)S, (Mg, Mn)S and (Mg, Fe)S solid solutions with the cubic (B1) structure [11], using the x-ray absorption spectroscopy results to study the phase transition of FeS in $Mg_{1-x}Fe_xS$ solid solution [12]. We also investigated the electronic structure of MeS (Me = Ca, Mg, Fe, Mn) monosulfides by S K- and L-edge x-ray absorption spectroscopy and theoretical full multiple-scattering calculations [13]. Very recently, S K-edge XANES spectroscopy was used to study phase transformation in $Fe_{1-x}S$ after ball milling [14]. Also, in early research, x-ray photoelectron spectroscopy was applied to the analysis of occupied electronic states in transition metal (TM) monosulfides [15].

The S K-edge XANES of FeS, CoS and NiS measured in [2, 6, 10] differ significantly in peak positions and overall shape (spectral profile). In addition, interlaboratory differences exist in the measured spectra which are probably related to near-surface oxidation [10]. Transition metal (TM) sulfides are rather reactive in the presence of air and readily oxidized to sulfates in the near-surface region. In this study on B8 structure FeS, CoS and NiS our measurement procedures eliminated atmospheric contamination of the sample region probed by the S K- and L-edge XANES spectra.

Several theoretical studies [16–27] have been made on the electronic structure of transition metal monosulfides starting from MO analysis of a simple FeS_6 cluster [16, 17]. Using LDA band structure calculations local partial DOSs for the transition metal sulfides (including FeS and NiS) have been obtained [22]. For antiferromagnetic FeS the spin polarized local DOS [23] and recently the local partial DOS [24] have been calculated. Bulk and surface local DOS in a series of TM monosulfides with NiAs structure has been obtained using the DFT approach [25]. The Ni 3d and S 3p partial DOS in the antiferromagnetic NiS have been calculated within the local spin-density approximation [27]. But some details of electronic structure of TM sulfides remain controversial. Understanding is complicated by complex magnetic behaviour, metal–nonmetal transition, influence of vacancies on electron delocalization and phase transitions, and uncertainty in the nature of metal–metal interactions. Several early studies show that metallic character increases in the sequence $FeS < NiS < Co_{1-x}S$, while some recent investigations [22, 25] support another order—namely FeS–CoS–NiS. It is associated with progressive increase in covalence and decrease in metal 3d electron interaction energy. A key feature of the NiAs-type (B8) structure is the sharing of the MS_6 (M = Fe, Co, Ni) octahedral faces along the *c*-axis which permits both a direct metal–metal interaction via either metal $3d(t_{2g})$ or metal $3d(e_g)$ orbitals and an indirect metal–sulfur–metal interaction via hybridized sulfur 3p (or sulfur 3d) and metal $3d(e_g)$ orbitals.

X-ray absorption near-edge structure (XANES) spectra yield information on unoccupied electron states, providing a partial map of the lower part of the conduction band. For the present monosulfides, this information is reflected similarly in both metal and sulfur K- and $L_{2,3}$-edge XANES due to the extensive mixing of unoccupied sulfur and metal electron states. For example, although transition of 1s core electrons to unoccupied 3d states is forbidden by the quantum selection rules in the electric dipole approximation [23], it becomes weakly to strongly allowed in metal sulfides through hybridization of unoccupied sulfur 3p σ^* antibonding and metal 3d (predominantly e_g) states [16]. This p–d hybridization is particularly strong for transition to $3d(e_g)$ states and, of course, covalent metal–S bonds, and accounts for the prominent edge feature of sulfur K-edge XANES spectra of the NiAs-type monosulfides of Fe, Co and Ni. A progressive increase in area of the edge peak of sulfur K-edge XANES in the sequence from $Fe_{0.923}S$ to $Ni_{0.923}S$ and $Co_{0.923}S$, attributed to progressive increase in the

number and availability of empty e_g (minority spin) orbitals and covalence of metal–S bonds, has been found [10].

Energy level diagrams for TM cations coordinated by anions (sulfur in the present case) generally predict strong hybridization between anion p symmetry orbitals and cation d-like levels. Thus, one can expect that changes in behaviour of d-like levels will be projected onto the p-like DOS. In our case, examining the S K absorption edge gives us information about unoccupied states above the Fermi energy. In the dipole approximation the sulfur K edge is generated by unoccupied S p states, while the S $L_{2,3}$ edge is formed by the unoccupied sulfur s and d states. So, analysis of the shape of the S K absorption edge (through the S p–TM d states hybridization effect) can also give the information on the TM cation d-like electrons, while analysis of the S $L_{2,3}$ XANES provides an opportunity to study the distribution of sulfur s and d states in the conduction band of the compounds.

In this study, we measure the S K- and $L_{2,3}$-edge XANES of NiS and CoS, perform their theoretical analysis on the basis of the full multiple-scattering approach and calculate the local partial DOS for these compounds. To our knowledge these are the first measurements of the S $L_{2,3}$-edge XANES spectra of NiS and CoS.

2. Experimental details

Samples were prepared from high-purity elements by dry reaction within evacuated sealed silica glass tubes. Stoichiometric FeS, NiS and CoS were prepared by direct reaction of S and hydrogen-reduced (∼900 °C) Fe, Ni and Co sponge, respectively, at 450 °C overnight, 600 °C for 1 day and 700 °C for 2 days. Because stoichiometric amounts of Co and S yielded a two-phase ($Co_{1-x}S$ + ∼Co_9S_8) mixture, all three monosulfides were prepared metal deficient (i.e. $(Fe, Co, Ni)_{0.923}S$) by reaction of appropriate molar proportions of FeS, NiS, CoS and S at 800 °C for two days, and the charges were quenched in water.

Sulfur K- and $L_{2,3}$-edge XANES spectra were collected at the Canadian Synchrotron Radiation Facility (CSRF), Aladdin storage ring (University of Wisconsin at Madison, WI), using a double-crystal monochromator (DCM) beamline and Mark IV Grasshopper monochromator beamline, respectively, in both total electron yield (TEY) and fluorescence yield (FY) modes as a function of incident photon energy [28]; both beamlines actually collect the current yield (CY) but this has traditionally been referred to as 'TEY'. The DCM is described elsewhere [29]; it uses an InSb(111) crystal, and has an energy resolution of about 0.6 eV (FWHM) at 1840 eV, and the Darwin width of the crystal corresponds to an energy resolution of 0.9 eV for the sulfur K edge. The Grasshopper beamline has been described previously [30]; it uses an 1800 mm^{-1} holographic grating with an energy resolution of <0.1 eV in the S L-edge region. For the L-edge measurements, sample preparation, including opening of the sample tubes, and transfer into the experimental chamber of the Grasshopper were performed in a nitrogen-filled glove bag attached to the port of the spectrometer sample chamber. All spectra were calibrated to the K- or L_3-edge peak of native sulfur at 2472.0 and 162.5 eV [31, 32], respectively, after removal of a linear pre-edge background. Other details of beamlines and procedures for measurement of spectra and data reduction are similar to those described and discussed in [10, 11, 13].

3. Method of calculation

The computer code G4XANES [33] was used in the present research for S K and $L_{2,3}$ XANES calculations. For comparison purposes, we also made simulations of the S K-edge XANES

of the studied sulfides with NiAs-type structure using the FEFF8.2 package [34] based on the self-consistent Hedin–Lundqvist potential. This package was also used for calculation of local densities of states of the sulfides.

In the G4XANES package atomic charge densities were obtained with the help of a self-consistent Dirac routine. Phase shifts of the photoelectron were calculated in the framework of the crystal muffin-tin (MT) potential scheme with touching MT spheres. The MT radii and the MT constants were obtained according to an established procedure of MT potential construction [33]. The MT approximation according to the Mattheiss prescription [35] was used while constructing the crystal potential.

It is well known [36] that within the dipole approximation the x-ray absorption coefficient, $\alpha(E)$, for the S K edge is given by

$$\alpha(E) = |m_{\mathrm{L}}(E)|^2 N_{\mathrm{p}}^{\mathrm{S}}(E), \tag{1}$$

where $N_{\mathrm{p}}^{\mathrm{S}}(E)$ is the partial density of unoccupied S states with p symmetry and $m_{\mathrm{L}}(E)$ is the normalized dipole transition matrix element given by

$$m_{\mathrm{L}}(E) = \frac{\int \mathrm{d}r \cdot \Phi_l(r, E) \cdot \Delta(r) \cdot \Psi_{\mathrm{c}}(r)}{\left[\int \mathrm{d}r \cdot \Phi_l^2(r, E)\right]^{1/2}}, \tag{2}$$

where $\Phi_l(r, E)$ is a solution of the radial Schrodinger equation at energy E for MT potential ($l = 1$ for the K edge), $\Delta(r)$ is the electron–photon interaction operator and $\Psi_{\mathrm{c}}(E)$ is the core K-level wavefunction. In the calculation, phase shifts with orbital momentum (l) up to 3 have been included.

For the S $L_{2,3}$-edge XANES, the situation is more complicated. There are two dipole allowed channels (p $\rightarrow$ d and p $\rightarrow$ s). We have calculated the S L_3 edge as a sum of partial p $\rightarrow$ s and p $\rightarrow$ d cross-section. The S $L_{2,3}$ edge has been obtained as a superposition of the S L_2 and S L_3 edges shifted by the value of spin–orbit splitting of 1.1 eV. It is well known that the spin–orbit interaction changes the L_2/L_3 branching ratio for several transition metal $L_{2,3}$ edges from 1:2 (see, for example, [37]), and several theoretical approaches have been suggested to estimate this ratio theoretically [38, 39]. But according to our knowledge there is no indication in the literature of a significant deviation of the branching ratio from 1:2 for the sulfur $L_{2,3}$ edge. That is why (as the exact value of branching ratio for the S $L_{2,3}$ edges in the compounds under the study is not known) we tried the 1:2 ratio (L_2:L_3) with quite reasonable results for the superimposed sulfur L_2 and L_3 edges.

In order to perform a direct comparison with experimental data one must take into account two factors. One factor is the filling of the occupied states following the Fermi distribution. The other factor is the broadening of experimental spectra due to the core hole lifetime, the finite mean free path of the photoelectron, and the experimental resolution. For the bandwidth of the core hole, we used 0.59 eV for the S K-edge XANES and 0.05 eV for the S $L_{2,3}$-edge XANES. The energy dependent function obtained in [36] was used for the mean free path of the photoelectron. The experimental energy resolutions are 0.9 eV for S K-edge XANES and $\sim$0.1 eV for the S $L_{2,3}$-edge XANES. All these factors contribute to the imaginary part of a complex MT potential.

In addition, one must compare the experimental data with the theoretical calculation made using a relaxed potential (i.e., taking into account the presence of the core hole). This effect was treated in the $Z+1$ approximation [40]. In our previous studies of other XANES we found that generally the K-edge XANES is less sensitive to the type of potential used (with core hole or ground state) than $L_{2,3}$-edge XANES. But in the present study including the core hole in the form of the $Z + 1$ approximation does not change significantly the shape of both the S K-edge and the S $L_{2,3}$-edge XANES.

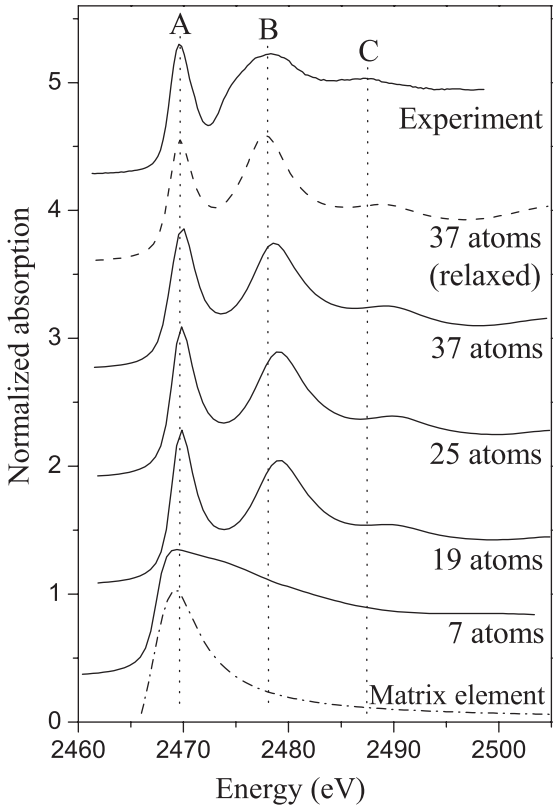

Figure 1. The comparison of the experimental S K XANES of NiS with the theoretical spectra calculated by the program code G4XANES for different sizes of cluster. The calculations have been made using the ground state potential. All spectra are aligned relative to the position of peak A of the experimental spectrum.

4. Results and discussion

An important step in the multiple-scattering analyses of XANES data is the determination of the minimum size of the cluster of neighbour atoms around the absorbing S atom within which the scattering of the photoelectron can reproduce all fine details of the experimental XANES. So, the dependence of the shape of the theoretical S K XANES on the cluster size has been investigated for all three TM monosulfides. It was shown recently [13] that the XANES spectrum for the S K edge in FeS with hexagonal NiAs-type structure results from the multiple scattering of an excited photoelectron inside a relatively small cluster of four shells (37 atoms). In figure 1 we present the comparison of the experimental S K XANES spectrum for one of the studied monosulfides, NiS, with the theoretical simulations carried out in ground state potential for different sizes of cluster. Theoretical spectra are aligned relative to the position of peak A of the experimental spectrum. The zero value of the muffin-tin energy is chosen to be the origin of the energy scale. One can see that the S K-edge XANES spectrum (figure 1) consists of a single broad maximum and differs significantly from the experimental spectrum for the cluster including only the first coordination shell (seven-atom cluster). But the spectrum calculated for a cluster of two coordination shells (19 atoms) is already in agreement with the experimental one and reproduces all of its features (A, B, C). Addition of the next coordination shells does not lead to significant change in the shape of the spectrum.

In the case of x-ray absorption it is necessary to keep in mind that the absorbing atom is no longer in the ground state. And one needs to use the potential of the excited state for XANES calculation. So, in figure 1 we also show the S K XANES spectrum of NiS calculated

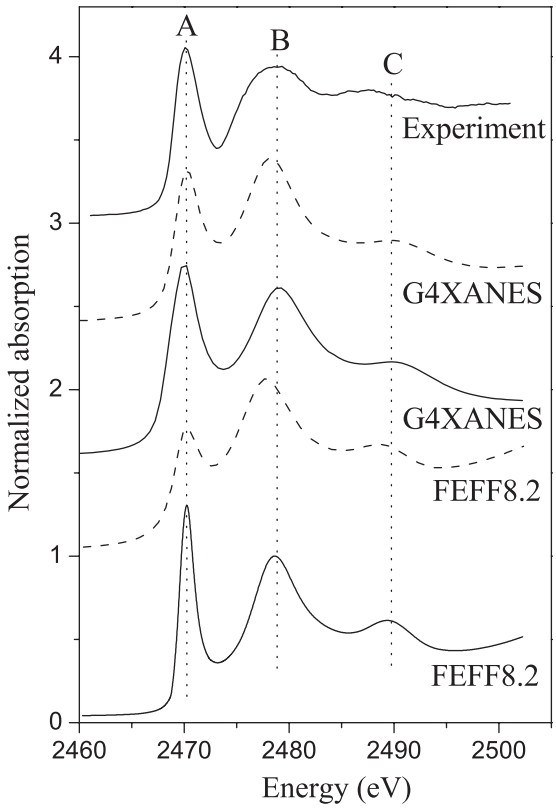

Figure 2. Comparison of the experimental S K XANES of CoS with theoretical simulations done by G4XANES code and FEFF8.2 code. The theoretical spectra were calculated in both ground state potential (solid curves) and relaxed potential (dashed lines). The cluster of four shells (37 atoms) was taken into consideration for calculations.

within a potential of the core hole using the $Z + 1$ approximation (dashed line). In the case of NiS it was found that the spectrum calculated within the $Z + 1$ approximation (dashed line in figure 1) is not in better agreement with the experiment. This finding means that one can use the experimental x-ray absorption spectra to study unoccupied electronic states in the conduction band, as the transition matrix element is a smooth function of the energy having no extra features (see figure 1).

For comparison purposes, we made calculations of the S K-edge XANES of the investigated sulfides (FeS, CoS and NiS) using the FEFF8.2 package based on the self-consistent Hedin–Lundqvist exchange potential. It was found that the results obtained using the FEFF8.2 program code are close to those obtained by our method using G4XANES code. As an example, in figure 2 the experimental S K XANES spectrum of CoS with NiAs-type structure is compared with theoretical spectra calculated using both G4XANES and FEFF8.2 packages.

The experimental S K XANES of iron, cobalt and nickel monosulfides are compared with the theoretical S K XANES calculated using the G4XANES code with the ground state potential in figure 3. The theoretical spectra were calculated for a cluster of four coordination shells (37 atoms). From figure 3 one can see a progressive increase in the intensity of the edge peak A of the experimental spectrum in the sequence FeS to NiS to CoS. The same behaviour is observed in the theoretical spectra. The progressive shift of features B and C to the high energy region in the sequence FeS to NiS to CoS is observed in both experimental and theoretical spectra. This observation is in agreement with Natoli's rule [41] which states that for solids of the same crystal structure type there is a simple relation between lattice spacing, R,

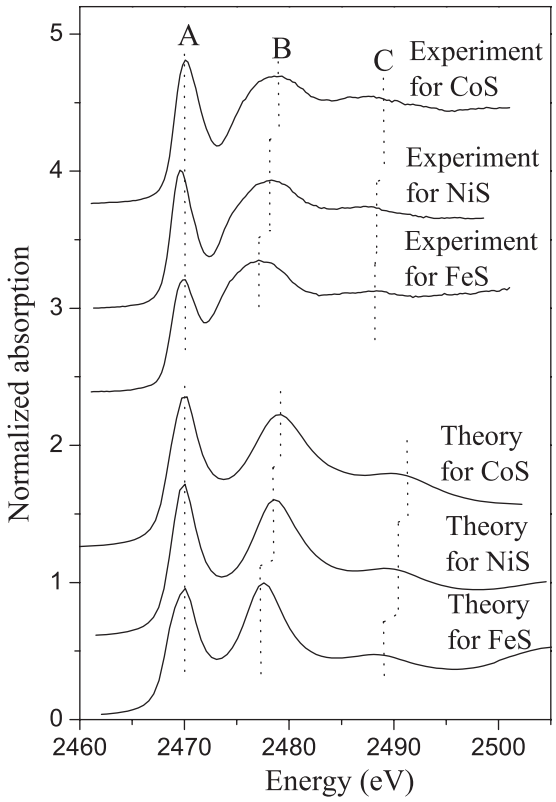

Figure 3. Comparison of the experimental S K XANES spectra for FeS, CoS and NiS with the corresponding theoretical spectra calculated by the program G4XANES for a cluster size of four shells (37 atoms) using the ground state potential.

and relative energy of corresponding XANES peaks, ΔE; namely $(R^2\Delta E) = \text{constant}$. The lattice parameters a and c decrease in the sequence FeS to NiS to CoS, so, the relative energies of peaks B and C increase. Thus, if one rescales the energy scale of NiS and CoS XANES by the factor $(R_{\mathrm{TMS}}/R_{\mathrm{FeS}})^2$ the resulting spectra should be identical to the spectrum of FeS.

A multiple-scattering approach within a muffin-tin approximation was applied previously to calculate the sulfur K-edge XANES of FeS, CoS and NiS crystals with the hexagonal NiAs-type (B8) structure [4]. But there was a significant difference between the calculated [4] and experimental spectra [2]; the energy separation between peaks was larger for the theoretical spectra, and the two principal peaks in the spectra of FeS and CoS were calculated to have intensity ratios opposite to those of the experimental spectra. The theoretical results reported in the present paper are in better agreement with the experimental spectra. From figure 3 one can see that the energy positions of peaks of the theoretical spectra for all three compounds are in good agreement with the experimental spectra, as are the intensity ratios of the first (A) and second (B) absorption peaks.

As noted above, the experimental S K XANES for FeS, CoS and NiS with the NiAs-type structure have been measured in previous studies [2, 6, 10], but these spectra differ from one laboratory to another for a given compound. The S K XANES spectra reported in the present paper resemble those presented in [2] and [10], but disagree with the spectra measured by Zajdel *et al* [6]. In the spectra of Zajdel *et al* [6], there is a prominent peak at ∼12 eV above the edge, that is not observed in either the currently reported spectra or the spectra of [2] and [10]. Farrell and Fleet [10] suggested that this additional peak was sulfate sulfur from

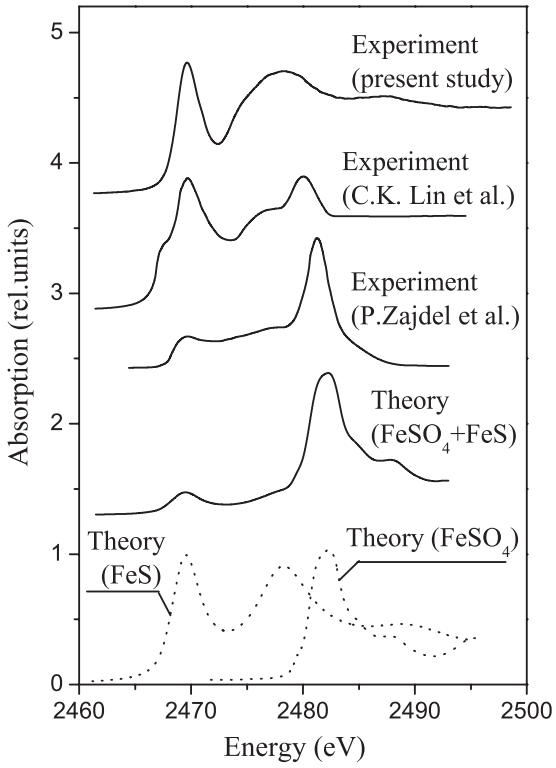

Figure 4. Comparison of the experimental S K XANES of FeS from different studies with model calculations (see text).

oxidation of the samples. To verify this suggestion we have made theoretical simulations of the S K edge of $FeSO_4$ and then summed this spectrum with the spectrum of FeS (see figure 4) using relative weights of 2:1. Clearly, the resulting profile agrees well with the experimental spectrum of Zajdel *et al* [6]. We also note that an extra peak at a similar location ($\sim$12 eV above the edge) was observed recently in the S K-edge XANES of non-stoichiometric $Fe_{1-x}S$ obtained by a mechanical ball-milling procedure [14].

Based on the agreement between the theoretical and experimental S K XANES spectra (figure 3), we conclude that our theoretical method works well and more complicated calculations for S $L_{2,3}$ XANES for studied compounds can now be attempted. In figure 5 we report the S $L_{2,3}$ XANES for NiS, comparing the experimental S $L_{2,3}$ absorption spectrum for NiS with theoretical spectra calculated for different cluster sizes using the ground state potential. The spectrum calculated in fully relaxed potential within the $Z + 1$ approximation is also shown in the figure. To our knowledge, these are the first theoretical calculations of S $L_{2,3}$ absorption spectra. From figure 5 one can see that all main details of the experimental spectra are reproduced for a relatively small cluster of two coordination shells (19 atoms). Addition of subsequent shells only results in insignificant changes in relative peak intensity. The calculation taking into account the fully relaxed potential (dashed line in figure 5) does not differ significantly from XANES spectra calculated in the ground state potential.

The experimental S $L_{2,3}$ XANES spectra for B8 structure FeS, CoS and NiS are shown in figure 6, and compared with the respective theoretical S $L_{2,3}$-edge absorption spectra. Similarly to the currently reported S K XANES spectra, the S $L_{2,3}$-edge spectra exhibit a progressive shift of peaks B, C and D toward the high-energy region which can be attributed to the change in the crystal lattice parameters (Natoli's rule).

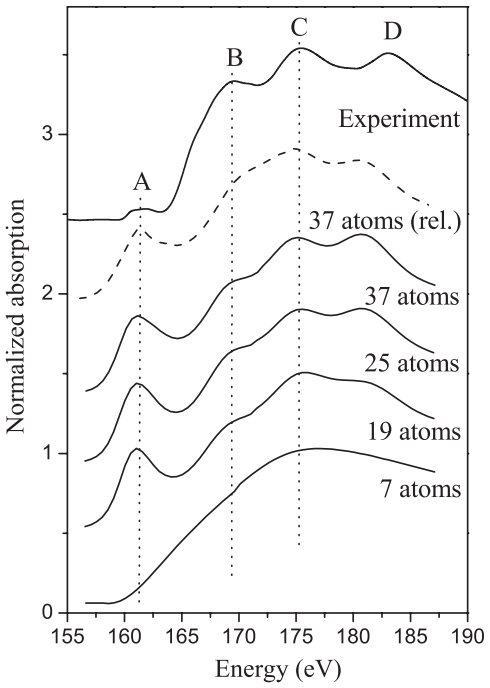

Figure 5. The experimental S $L_{2,3}$ XANES spectrum of NiS with NiAs-type structure compared with theoretical spectra calculated for different cluster sizes using the ground state potential. The spectrum calculated in fully relaxed potential within the $Z+1$ approximation is shown by a dashed line. The G4XANES package was used to calculate spectra.

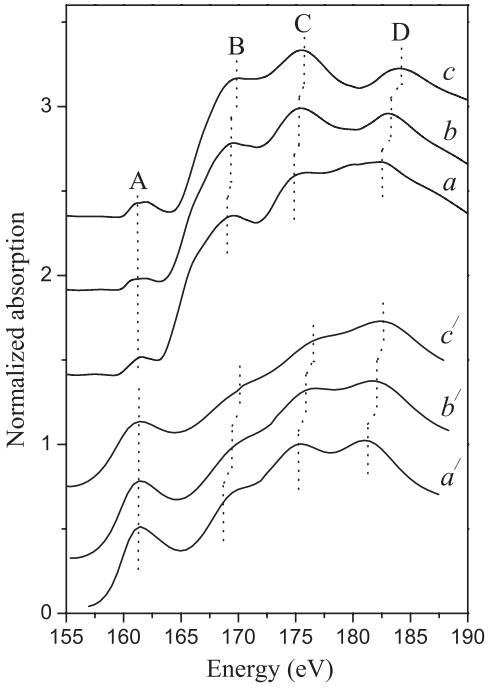

Figure 6. The experimental S $L_{2,3}$ XANES for FeS (curve a), NiS (curve b) and CoS (curve c) having NiAs-type structure. Curves a', b' and c' correspond to the theoretical S $L_{2,3}$ XANES for FeS, NiS and CoS, respectively. The theoretical spectra were calculated by the program G4XANES for the cluster size of four shells (37 atoms) using the ground state potential.

We next use the x-ray absorption spectra to investigate the electronic structures of NiS and CoS. The agreement between theoretical and experimental spectra obtained for both K-edge and $L_{2,3}$-edge XANES shows that the theoretical approach used in the present study is valid for the description of the electronic structure of the compounds under the study. It was found previously [13] on the basis of spin-dependent partial DOS analysis that for FeS there is almost no change in the shape of the corresponding spin-up and spin-down DOSs except slight modifications of the Fe d states and S p states. In the present study we have calculated the curves proportional to the projected electronic DOS of NiS and CoS calculated using the FEFF8.2 code. The calculations have been done using the ground state potential with the NOHOLE control card. To study the importance of the spin-polarization effect on the local partial DOS of CoS we have performed the calculation using a spin-polarized approach. The results for CoS are presented in figure 7. As one can see, there are only slight modifications in the shape of Co d states and small energy shifts of other DOSs for spin-up and spin-down DOSs.

Figure 8 shows the Ni d and S p DOS in the valence band of NiS calculated for a cluster of 170 atoms. Analysis of hybridized Ni d–S p states shows that along with 'normal' hybridization of admixture type (where the maximum of one partial DOS corresponds to the maximum of another partial DOS) in the energy region of the main Ni d DOS peak (between dashed lines A and B) there is a second type of hybridization. In this second case the density of S p states is

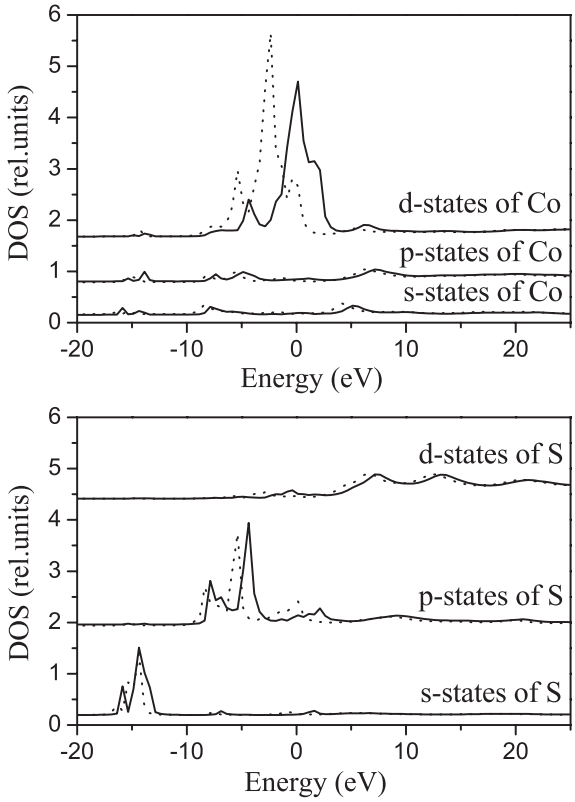

Figure 7. Local partial spin-polarized density of unoccupied electron states for CoS. The origin of the energy scale corresponds to the Fermi level. Spin-down DOSs are shown by solid curves, spin-up DOSs by dotted curves.

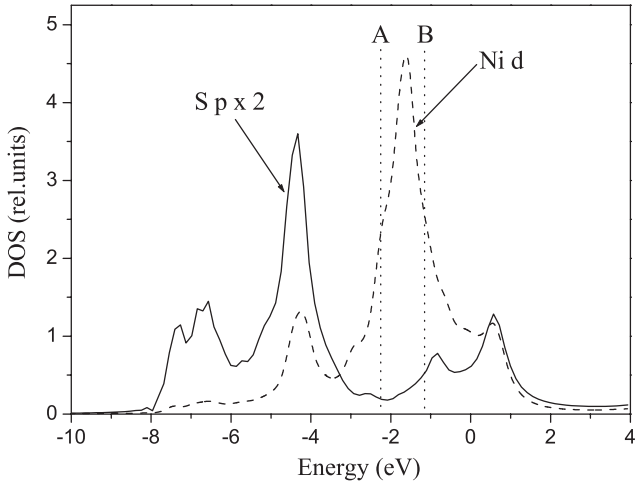

Figure 8. The Ni d and S p densities of electronic states in the valence band of NiS. The calculations are for a cluster size of 170 atoms. The origin of the energy scale corresponds to the Fermi level. The S p DOS is multiplied by a factor of two.

pushed away from the interval of Ni d states. For the unoccupied states such specific interaction between electronic states has been previously found for rare earth sulfides [42], CeO_2 [43], orthoferrites [44] and stishovite [45]. Thus, one may conclude that in this energy region the interaction between S p states and Ni d states has repulsive character.

From the theoretical local partial DOS one can estimate the energy distance between the highest peaks in the sulfur p and TM 3d bands and this parameter can be considered to be a

Table 1. The local partial charges obtained as a result of FEFF self-consistent calculation.

Orbital momentum	CoS		NiS	
	Co	S	Ni	S
s	0.534	1.776	0.554	1.812
p	0.747	3.707	0.732	3.809
d	7.831	0.407	8.772	0.322

measure of the covalence of the bonding in these compounds. We estimate these values to be 3.52 eV for FeS, 3.50 eV for CoS and 2.9 eV for NiS. Thus according to the present findings the covalence character of the chemical bonding increases in the series FeS → CoS → NiS, which is in agreement with some recent studies [22, 25].

Through the series of TM sulfides FeS → CoS → NiS, the number of 3d electrons increases (see table 1) and, correspondingly, the unoccupied part of the TM 3d band decreases. The widths of the unoccupied part of the TM 3d band estimated at half maximum height are 1.04 eV for FeS, 0.92 eV for CoS and 0.74 eV for NiS (relative values being 1.0:0.91:0.73). The associated shift of the Fermi level must result in an increase of sulfur occupied states (see table 1) and a corresponding decrease in the unoccupied part of the sulfur p states. The widths of the first peak of the experimental S K-edge XANES are 3.3 eV for FeS, 3.1 eV for CoS and 2.6 eV for NiS, the relative values being 1.0:0.94:0.78, very close to those obtained in the above theoretical TM 3d DOS analysis.

5. Conclusions

Combined x-ray absorption spectroscopic and theoretical full multiple scattering analysis made it possible to study fine details of the electronic structure of transition metal monosulfides. One can use the experimental S K-edge x-ray absorption spectra to study sulfur p unoccupied electronic states in the conduction band of TM monosulfides. The covalence character of the chemical bonding increases in the following series: FeS → CoS → NiS. A special type of hybridization where the density of S p states is pushed away from the interval of Ni d states is found in NiS along with 'normal' hybridization of admixture type (where the maximum of one partial DOS corresponds to the maximum of another partial DOS).

Acknowledgments

We thank K H Tan and Astrid Jorgensen, Canadian Synchrotron Radiation Facility, and staff of the Synchrotron Radiation Centre (SRC), University of Wisconsin, for their technical assistance, and the National Science Foundation (NSF) for the support of the SRC under grant no DMR9212658. This work was supported by the Natural Sciences and Engineering Research Council of Canada.

References

[1] Sugiura C 1981 *J. Chem. Phys.* **74** 215
[2] Sugiura C, Gohshi Y and Suzuki I 1974 *Phys. Rev.* B **10** 338
[3] Sugiura C 1984 *J. Chem. Phys.* **80** 1047
[4] Kitamura M, Sugiura C and Muramatsu S 1988 *Solid State Commun.* **67** 313

[5] Womes M, Karnatak R C, Esteva J M, Lefebvre I, Allan G, Olivier-Fourcade J and Jumas J C 1997 *J. Phys. Chem. Solids* **58** 345
[6] Zajdel P, Kisiel A, Zimnal-Starnawska M, Lee P M, Boscherini F and Giriat W 1999 *J. Alloys Compounds* **286** 66
[7] Pong W F, Mayanovic R A, Wu K T, Tseng P K, Bunker B A, Hiraya A and Watanabe M 1994 *Phys. Rev.* B **50** 7371
[8] Lawniczak-Jablonska K, Iwanowski R J, Goacki Z, Traverse A, Pizzini S, Fontaine A, Winter I and Hormes J 1996 *Phys. Rev.* B **69** 1119
[9] Nakamura M, Fujimori A, Sacchi M, Fuggle J C, Misu A, Mamori T, Tamura H, Matoba M and Anzai S 1993 *Phys. Rev.* B **48** 16942
[10] Farrell S P and Fleet M E 2001 *Phys. Chem. Miner.* **28** 17
[11] Farrell S P, Fleet M E, Stekhin I E, Kravtsova A, Soldatov A V and Liu X 2002 *Am. Mineral.* **87** 1321
[12] Kravtsova A N, Stekhin I E, Soldatov A V, Liu X and Fleet M E 2002 *Phys. Status Solidi* b **234** R4
[13] Kravtsova A N, Stekhin I E, Soldatov A V, Liu X and Fleet M E 2004 *Phys. Rev.* B **69** 134109
[14] Lin C K, Du C L, Chen G S, Louh R F, Lee P Y and Lin H M 2004 *Mater. Sci. Eng.* A **375–377** 834
[15] Gopalakrishnan J, Murugesan T, Hegde M S and Rao C N R 1979 *J. Phys. C: Solid State Phys.* **12** 5255
[16] Tossell J A 1977 *J. Chem. Phys.* **66** 5712
[17] Sakkopoulos S, Vitoratos E and Argyreas T 1984 *J. Phys. Chem. Solids* **45** 923
[18] Marfunin A S 1979 *Physics of Minerals and Inorganic Compounds* (Berlin: Springer)
[19] Sakkopoulos S, Vitoratos E and Argyreas T 1986 *J. Chem. Educ.* **63** 665
[20] Tossell J A and Vaughan D J 1992 Theoretical geochemistry: applications of quantum mechanics *Earth and Mineral Sciences* (New York: Oxford University Press)
[21] Anzai S 1997 *Physica* B **237/238** 142
[22] Raybaud P, Hafner J, Kresse G and Toulhoat H 1997 *J. Phys.: Condens. Matter* **9** 11107
[23] Hobbs D and Hafner J 1999 *J. Phys.: Condens. Matter* **11** 8197
[24] Rohrbach A, Hafner J and Kresse G 2003 *J. Phys.: Condens. Matter* **15** 979
[25] Gomez-Balderas R, Oviedo-Roa R, Martinez-Magadan J M, Amador C and Dixon D A 2002 *Surf. Sci.* **518** 163
[26] Toulhoat H, Raybaud P, Kasztelan S, Kresse G and Hafner J 1999 *Catal. Today* **50** 629
[27] Koutti L and Hugel J 1999 *J. Phys.: Condens. Matter* **11** 1979
[28] Bancroft G M 1992 *Can. Chem. News* **44** 15
[29] Yang B X, Middleton F H, Olsson B G, Bancroft G M, Chen J M, Sham T K, Tan K and Wallace D J 1992 *Phys. Res.* A **316** 422
[30] Tan K H, Bancroft G M, Coatsworth L L and Yates B W 1982 *Can. J. Phys.* **60** 131
[31] Fuggle J C and Inglesfield J E 1992 *Unoccupied Electronic States: Fundamentals for XANES, EELS, IPS and BIS* (New York: Springer)
[32] Weast R C, Astle M J and Beyer W H 1986 *CRC Handbook of Chemistry and Physics* (Boca Raton, FL: CRC Press)
[33] Della Longa S, Soldatov A V, Pompa M and Bianconi A 1995 *Comput. Mater. Sci.* **4** 199
[34] Ankudinov A L, Ravel B, Rehr J J and Conradson S 1998 *Phys. Rev.* B **58** 7565
[35] Mattheiss F 1969 *Phys. Rev.* **181** 987
[36] Muller J E, Jepsen O and Wilkins J W 1982 *Solid State Commun.* **42** 365
[37] Fink J, Muller-Heinzerling T, Scheerer B, Speier W, Hillebrecht F U, Fuggle J C, Zaanen J and Sawatzky G A 1985 *Phys. Rev.* B **32** 4899
[38] Schitalla J and Ebert H 1998 *Phys. Rev. Lett.* **80** 4586
[39] Ankudinov A L, Nesvizhskii A I and Rehr J J 2003 *Phys. Rev.* B **67** 115120
[40] Durham P J 1988 *X-ray Absorption: Principles, Applications and Techniques of EXAFS, SEXAFS and XANES* ed R Prins and D C Koningsberger (New York: Wiley) p 53
[41] Bianconi A 1988 XANES spectroscopy *X-ray Absorption: Principles, Applications and Techniques of EXAFS, SEXAFS and XANES* ed R Prins and D C Koningsberger (New York: Wiley) p 573
[42] Soldatov A V and Gusatinskii A N 1984 *Phys. Status Solidi* b **125** k129
[43] Soldatov A V, Ivanchenko T S, Della Longa S, Kotani A, Iwamoto Y and Bianconi A 1994 *Phys. Rev.* B **50** 5074
[44] Povahznaja N A, Shvejtzer I G and Soldatov A V 1995 *J. Phys.: Condens. Matter* **7** 53
[45] Soldatov A V, Kasrai M and Bancroft G M 2000 *Solid State Commun.* **115** 687